KOMPLEKSOWY PRZEGLĄD METOD PREPARATYKI, WŁAŚCIWOŚCI I ZASTOSOWAŃ FOTOKATALITYCZNYCH RÓŻNYCH STRUKTUR PEROWSKITOWYCH

A COMPREHENSIVE REVIEW OF PREPARATION METHODS, PROPERTIES, AND PHOTOCATALYTIC PERFORMANCE OF DIVERSE PEROVSKITE STRUCTURES

Magdalena Miodyńska[1], Onur Cavdar[1], Anna Pancielejko[1],*

[1]*Department of Environmental Technology, Faculty of Chemistry, University of Gdansk, 80-308 Gdansk, Poland*
*e-mail: anna.pancielejko@ug.edu.pl

Dr Magdalena Miodyńska completed her bachelor's studies (2012-2015) and subsequently her master's studies (2015-2017) in Chemistry with a specialization in analytical and chemical diagnostics at the Faculty of Chemistry, University of Gdańsk. In 2023, she earned a doctoral degree in chemical sciences upon completing the Stationary Doctoral Studies in Chemistry and Biochemistry at the Faculty of Chemistry, University of Gdańsk. Her expertise lies in synthesizing new materials with enhanced photocatalytic activity for reactions aimed at degrading environmental pollutants and in reactions focused on producing molecular hydrogen as a clean energy source. She is a co-author of numerous scientific articles published in reputable scientific journals.

https://orcid.org/0000-0001-7273-3252

Dr Onur Cavdar earned his B.Sc. degree from Faculty of Chemistry and Metallurgy, Chemical Engineering Department, Yıldız Technical University in Istanbul, Türkiye in 2016. He obtained his master's degree from the Faculty of Chemistry, Gdańsk University of Technology, Poland under the supervision of Professor Justyna Łuczak in 2018. In the same year, he started his PhD studies in the Photocatalysis Group in Faculty of Chemistry, University of Gdańsk, Poland under the supervision of Professor Adriana Zaleska-Medynska and he obtained his PhD degree in 2023.

Onur Cavdar is currently working as a postdoctoral researcher in the University of Gdańsk in the EU funded project "H$_2$OforAll" aiming at developing innovative water treatment methods to remove disinfection byproducts (DBPs) using adsorption and photocatalytic technologies.

https://orcid.org/0000-0002-7626-3881

Dr Anna Pancielejko received her PhD (2022) degree from Gdansk University of Technology. Currently, she works as a postdoctoral fellow (2022–2024) at the University of Gdansk. Her research interests include developing photoactive nanomaterials such as oxides, perovskites, and metal-organic frameworks for energy and environmental applications.

https://orcid.org/0000-0002-2184-1912

ABSTRACT

Perovskite materials for photocatalytic environmental and energy conversion applications have drawn excessive attention over recent years owing to their unique photoelectric and catalytic properties. As harvesting solar energy within the bounds of possibility is one of the main aims of photocatalysis, many research groups have devoted their efforts to developing perovskite-based photocatalytic materials from perovskite oxide to metal halide and double halide-based perovskite materials with various synthesis strategies. Particularly, halide and double halide-based perovskites are intriguing thanks to their tunable band gap and band structure depending on the type of halide. Apart from the obstacles related to charge separation and transport processes; instability under water, oxygen, and high temperature hindering their practical photocatalytic application are remaining challenges. Toxicity emerging from Pb^{2+} or Sn^{2+} release due to chemical instability is another concern to be tackled. Thus far, replacing Pb^{2+} or Sn^{2+} with Bi^{3+} is one of the current scopes in the perovskite photocatalysis area while ensuring chemical stability in halide-based perovskites and thus reducing toxicity. Despite all those challenges, the popularity of perovskite photocatalysis is growing amid the favorable light induced chemical reactions via a plentiful range of promising cost-effective manufacturing methods of perovskites. In this review, the principles and photocatalytic applications of the perovskite oxides, metal halide-based perovskites, and double halide-based are comprehensively discussed.

LIST OF ABBREVIATIONS AND SYMBOLS

AM 1.5G filter   - Air Mass filter modifies the spectral output of the arc lamp to match specific solar conditions
DMA   - dimethylammonium cation
EDTA   - ethylenediaminetetraacetic acid
FA   - formamidinium cation
GO   - graphene oxide
LARP   - ligand-assisted reprecipitation method
MA   - methylammonium cation
MeOH   - methanol
MO   - Methyl Orange
MR   - Methyl Red
RhB   - Rhodamine B
Sudan Red III   - lysochrome diazo dye
TC   - Tetracycline
QDs   - quantum dots
ZIFs   - zeolitic imidazolate frameworks
λ - wavelength (nm)

INTRODUCTION

Perovskites are crystalline materials characterized by an octahedral units based structure and renowned for their unique physicochemical properties, making them versatile in various branches of science and technology. The credit for the first discovery of the perovskite mineral goes to the mineralogist and crystallographer Gustav Rose. In 1839, Rose received a mineral sample from the Ural Mountains, courtesy of August Alexander Kämmerer, the Chief Mines Inspector of the Russian Empire. Subsequently, in the laboratory in Berlin, Rose conducted a thorough examination of the physical properties and chemical composition of the mineral, identified as $CaTiO_3$ [1]. The results of his investigation were documented in a scientific article [2]. In adherence to Kämmerer's suggestion, Rose coined the term "perovskite" to designate the newly characterized structure, paying homage to the Russian politician and mineralogist Count Lev Aleksevich Perovski. The nomenclature choice served not only to acknowledge Perovski's contributions but also to establish a standardized identification for this intriguing class of crystalline materials.

Rose's discovery in 1839 marked the commencement of a series of explorations and subsequent revelations concerning novel perovskite structures. These investigations also delved into the understanding of numerous desirable properties exhibited by these materials. Soon thereafter, a comprehensive classification of perovskites into oxygen-based, halide-based, and double halide perovskites emerged [3]. Regardless of the classification type, the crystalline structure of perovskites, featuring octahedral units, provides a conducive environment for the manifestation of effects such as ferroelectricity, ferromagnetism, and thermoelectricity [4,5]. Furthermore, halide perovskites, in most cases, belong to narrow band gap semiconductors, endowing them with the capability to absorb light within the solar radiation spectrum. This characteristic renders them appealing for photovoltaic applications [6]. In the realm of electronics, perovskites serve as the foundation for innovative integrated circuits, while in solar energy, they are gaining prominence as potentially efficient materials for photovoltaic cell production, displacing conventional silicon-based cells [7]. Additionally, their energy storage capabilities, magnetic properties, and thermoelectric characteristics open new horizons in the field of energy technologies and storage [8].

The future of perovskites appears exceptionally promising. Research on new types of perovskite structures, modifications to the crystalline framework, and innovative applications are evolving dynamically. Looking ahead, we envision the potential utilization of perovskites not only in the field of energy but also as pivotal components in quantum technology, optical communication, and nanotechnology.

The central theme of this review underscores the perovskites which have found successful applications in photocatalytic processes.

1. THE STRUCTURES AND PROPERTIES OF PEROVSKITE MATERIALS

1.1. PEROVSKITE OXIDES

Perovskite oxides (ABO_3) have been long known since the discovery of the $CaTiO_3$ mineral [9]. In the perovskite oxide structures, cation A often constitutes the alkali/alkaline earth elements that have a larger radius than that of the second cation in the perovskite structure B which is a d-block transition element [10]. The ideal crystal structure of ABO_3 is cubic where the cation A is surrounded by 12 oxygen atoms dodecahedrally while B is in an octahedral environment with 6 oxygen atoms [11]. However, the ideal cubic-structured ABO_3 deviates due to octahedral distortions [11,12]. Perovskite oxides possess a large variety of materials owing to the cation A and B interchangeability. Thus, perovskite oxides have drawn a lot of interest for a variety applications including gas sensors [13], optoelectronic [14], batteries [15], supercapacitors [16], catalytic [17] and photocatalytic applications [18].

Utilizing solar energy has an important role as part of the decarbonization efforts [19].Within this framework, semiconductor perovskite oxides photocatalysis is gaining significant attention in the photocatalysis community as a prominent candidate for highly active photocatalytic materials for a range of applications such as hydrogen production [20], water treatment [21], CO_2 conversion [22] and N_2 fixation [23]. Beyond the wide range of possibilities of materials and photocatalytic applications, perovskite oxides are appealing due to their remarkable stability which is a hallmark metal oxides [24]. This type of photocatalytic perovskite oxide materials can be obtained with various methods, such as solvothermal [25], hydrothermal [25,26], sonochemical [27], microwave-assisted hydrothermal [28], solid state [29], and pulsed laser ablation [30].

One of the examples of perovskite oxide photocatalysis is a n-type semiconductor $CaTiO_3$ with a band gap value of 3.5 eV which exhibits optical absorption in the UV region ($\lambda < 400$ nm) [31]. Like many photocatalytic materials, especially those with a large band gap, doping techniques with Cu [32] and Fe [33] are available for $CaTiO_3$ to improve visible light activity. Depending on the application, metal photodeposition is also an available option to enhance the photocatalytic activity [34,35].

As mentioned above in the provided $CaTiO_3$ example, doping in perovskite oxide materials can be carried out at three sites (A, B, and O-sites), which enhances their photocatalytic performance and boosts light absorption through band gap

change. The other issue that restricts the activity of all photocatalytic materials is the recombination of photogenerated charges. There are various approaches that can be used to overcome these two problems. One possibility is defect engineering, which involves creating controlled cation vacancies in perovskite oxide. Another option is heterojunction formation. In this approach, one perovskite oxide can be deposited with metal nanoparticles, combined with conducting materials such as graphene and other semiconductor materials in the right band position to create heterojunctions and composites that efficiently allow charge transfer across the newly formed interfaces [10].

There are numerous promising perovskite oxides where occasionally the cation A consists of different elements than alkali/alkaline earth elements as in $BiFeO_3$ [36] or $LaNiO_3$ [37]. Several examples of perovskite oxides with their application performances and conditions are given in Table 1. As is seen, many studies on perovskite oxides in photocatalysis exist in the literature aiming at the high activity owing to their compositional, stoichiometric, and structural flexibility. UV, IR, and visible light can all be harvested by photocatalysts based on perovskite oxides. However, one of the main concerns in the application of perovskite oxides on a larger scale is their stability. In general, it is considered that there are primarily two types of stability problems with perovskite oxides which are related with the intrinsic and extrinsic properties [9,38]. For instance, electronic band structure, thermodynamic phase stability, and structural stability are all components of intrinsic stability. While the oxidation/photo-oxidation of charge-transporting layers, light-induced ion redistribution, light stability, thermochemical stability, and interaction with water molecules and pathways of degradation can be attributed to the extrinsic stability problems [9,38]. If one desires to assert the potential for using perovskite oxide in photocatalysis, those limiting factors must be taken into consideration. In view of that, $SrTiO_3$ may be one of the most popular types of perovskite oxide due to its high activity and stability in photocatalytic full water splitting applications not only on the laboratory scale but also in large solar induced hydrogen evolution facilities [39]. Thanks to amazing work on this material in the form of $SrTiO_3$-Al loaded with Rh, Cr, and Rh species, which resulted in H_2 and O_2 evolution at the stoichiometric ratio under solar irradiation, this n-type semiconductor photocatalysis with the band gap value of approximately 3.2 eV has gained notoriety. [29,40].

1.2. HALIDE PEROVSKITES DERIVATES

A distinct subset within the perovskite class comprises halide perovskites characterized by the general formula ABX_3, where X represents Cl, Br, I, and their combinations. The B cations manifest as divalent entities (e.g., Pb^{2+} or Sn^{2+}), whereas the A cations consist of sizable, monovalent alkali metals (predominantly Cs) or

diminutive organic cations, such as methylammonium (MA) or formamidinium (FA). Deviations from the ABX₃ stoichiometry may arise through partial or complete vacancies in the positions of A and B cations (resulting in perovskites organized with vacancies) or through substitution with a combination of other cations (exhibiting varying valences yet maintaining overall charge neutrality), leading to the formation of double or quadruple perovskites. Nevertheless, a majority of perovskites demonstrate diminished symmetry due to lattice distortions, distorted octahedra, ordered cations, vacancies, or the inclusion of organic cations or inorganic clusters. Various structural permutations of perovskite architectures are illustrated in Figure 1 [41].
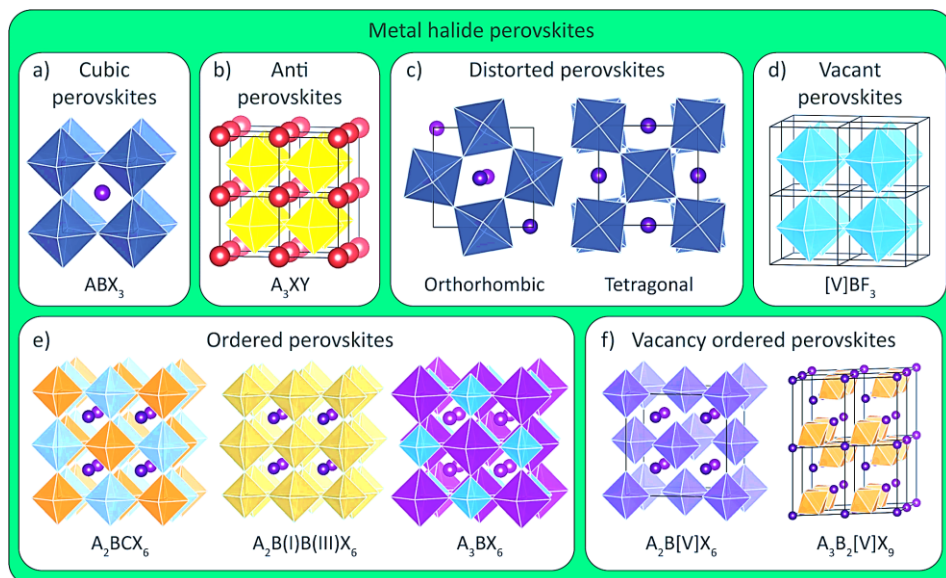

Figure 1.   Schematic representation of diverse perovskite crystal structures: a) conventional ABX₃ cubic halide perovskites; b) antiperovskites, characterized by A as a monovalent metal (e.g., Li⁺ or Ag⁺), X as a halide, and Y as a chalcogenide; c) orthorhombic and tetragonal disordered perovskites resulting from octahedral tilting; d) vacant BX₃ perovskites, exemplified by AlF₃; e) organized perovskites, wherein two M(II) metals are substituted by M(I) and M(III) metals; f) vacancy-ordered perovskites involving the replacement of a portion of B-site cations with M(III) or M(IV) metals and vacancies. Above figure is an adaptation of the figure from [41]. Copyright 2020 American Chemical Society

Rysunek 1.   Schematyczne przedstawienie różnorodnych struktur krystalicznych perowskitów: a) konwencjonalne sześcienne perowskity halogenkowe typu ABX₃; b) antyperowskity, w których A jest metalem jednowartościowym (np. Li⁺ lub Ag⁺), X oznacza halogenek i Y - chalkogenek; c) perowskity o nieuporządkowanym kształcie rombowym i tetragonalnym, powstałe w wyniku przechylenia oktaedrycznego; d) wolne perowskity BX₃, których przykładem jest AlF₃; e) zorganizowane perowskity, w których dwa jony M(II) są podstawione jonami metali M(I) i M(III); f) perowskity uporządkowane w oparciu o wakaty, polegające na zastąpieniu części kationów B metalami M(III) lub M(IV) i wakatami. Powyższy rysunek jest adaptacją rysunku z pracy [41]. Prawa autorskie należą do 2020 American Chemical Society

Materials classified as halide perovskites are considered highly promising due to their exceptional potential for converting light energy into electricity. Consequently, they have found numerous applications in photovoltaic cells and photodetectors [42]. Equally common is their utilization in light-emitting diodes (LEDs), lasers, and X-ray scintillators [43,44]. Moreover, owing to unique characteristics such as semiconductor behavior, a narrow band gap with appropriately positioned conduction and valence band edges, and a good absorption response in the visible light range, these materials have also been applied in photocatalytic reactions aimed at degrading environmental pollutants, generating clean energy carriers such as hydrogen, converting CO_2, or synthesizing organic compounds [45,46].

Unfortunately, a significant limiting factor for their widespread application is their high instability in contact with water or oxygen [47]. In the case of utilizing halide perovskites in photocatalytic reactions, modified systems are often encountered in the literature (by introducing dopants into the perovskite structure, depositing onto matrices such as semiconductor substrates, encapsulation in metal-organic frameworks, etc.), obtained to enhance the desired properties of perovskites or increase their stability. In the case of CO_2 photoreduction reactions, with CO and CH_4 as the main products, applied Fe(II)-doped $CsPbBr_3$ perovskite [48]. While the use of undoped perovskite resulted in the generation of CO as the main reaction product, Fe(II)-$CsPbBr_3$ exhibited dominance in CH_4 production. The authors associated the type of dominant product with the enhanced photoresponse of the doped perovskite and the altered adsorption/desorption capabilities of molecules on the photocatalyst surface. On the other hand, Kong et al. synthesized photocatalytic systems for CO_2 photoreduction of the core/shell type by fabricating zinc/cobalt-based zeolitic imidazolate frameworks (ZIFs) in the presence of $CsPbBr_3$ perovskite quantum dots [49]. This approach aimed primarily to enhance the perovskite stability in contact with moisture, increase CO_2 capture capacity, and improve charge separation efficiency. The authors confirmed the increased efficiency of the CO_2 photoreduction process when using hybrid perovskite/ZIF materials. However, a challenge arises in utilizing perovskites in photocatalytic reactions aimed at hydrogen generation, as traditional electrolytes in such processes have been aqueous solutions of methanol, glycerol, triethanolamine, and others. It is known that perovskite materials undergo hydrolysis in aqueous solutions, thus losing their properties. To address this, researchers employed a solution of concentrated halide acid, in which halide perovskites exhibit high stability. For instance, $(CH_3NH_3)_3Bi_2I_9$ perovskite was applied in the photocatalytic hydrogen generation process in an HI solution [50]. Furthermore, the authors demonstrated the stability of the system and the fact that additional modification of the perovskite with platinum nanoparticles as a co-catalyst resulted in almost a 14-fold increase in process efficiency. Due to the instability of perovskites in humid environments, they can be successfully applied as photocatalysts in the degradation of environmental pollutants present in the air. One of our recent studies involved encapsulating $Cs_3Bi_2Br_9$ with polythiophene, and the

obtained materials were successfully utilized for the degradation of toluene in the air [51]. The presence of a polymeric layer on the perovskite surface increased the adsorption of toluene molecules on the composite surface, protected the perovskite from photodestruction, and observed an improved flow of photocharges between the composite components, resulting in higher efficiency of pollutant degradation. However, the potential for using perovskites in photocatalytic processes is still immense and represents a challenge in the modern scientific world.

Traditional and widely recognized single halide perovskites of the $CsPbX_3$ type (where X denotes a halide anion/s) inherently incorporate toxic lead ions in their structure, posing potential environmental concerns upon material degradation and thus releasing lead cations [43]. The scientific response to this issue involves the utilization of related halide perovskites wherein the lead divalent cation is substituted with tin(II), germanium(II), bismuth(III), or antimony(III) cations [52]. Unfortunately, the facile oxidation of Sn^{2+} and Ge^{2+} to Sn^{4+} and Ge^{4+} induces a rapid deterioration in the photovoltaic characteristics of the respective perovskites [52]. Moreover, tin compounds exhibit toxicity, with well-established and documented adverse effects on both the environment and human health. In contrast, metals from the main group VA, such as bismuth and antimony, readily obtained from natural reservoirs, demonstrate heightened chemical stability in their trivalent states and exhibit reduced toxicity compared to Pb^{2+} and Sn^{2+} [52].

Among these alternative materials, Bi-based perovskites exhibit significant application potential due to their favorable physicochemical properties and high stability [53]. Capitalizing on their high absorption coefficient and pronounced solar light conversion efficiency, Bi–based perovskites have proven successful in applications such as solar cells [54] and photocatalytic reactions for hydrogen production [50,53,55,56], CO_2 conversion [57], and the degradation of environmental pollutants [58,59] (see Table 1).

1.3. DOUBLE HALIDE PEROVSKITES

Recently, there has been a notable increase in the importance of studying halide double perovskites. This increased attention is attributed to their enhanced stability and non-toxic nature compared to perovskites containing lead halides (Figure 2). Lead-free halide double perovskites, characterized by the general formula $A_2B'B''X_6$, signify an innovative class of perovskite materials. In this formula, the traditional Pb^{2+} ion is substituted with two distinct cations: a monovalent metal cation (such as Cs^+, MA^+, Ag^+) and a trivalent metal cation (Bi^{3+}, Sb^{3+}, In^{3+}). This strategic substitution facilitates the attainment of an average oxidation state of +2, aligning with that observed in lead halide perovskites. Moreover, the A-site typically accommodates larger cations, while the B' and B'' sites can host different cations

with distinct properties. The halide anion (Cl-, Br-, I-) is represented by X. This manipulation of the chemical composition broadens the scope of potential applications and improves the photocatalytic properties, adaptability, and versatility of halide double perovskite structures.
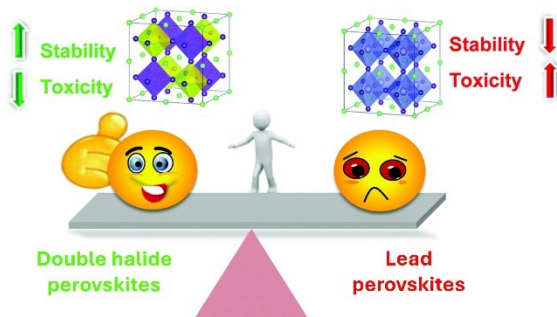

Figure 2. Distinctions between lead-free double perovskites and lead halide. Above figure is an adaptation of the figure from [60]. Copyright 2022 Royal Society of Chemistry

Rysunek 2. Porównanie bezołowiowych perowskitów podwójnych i perowskitów halogenkowo-ołowiowych. Powyższy rysunek jest adaptacją rysunku z pracy [60]. Prawa autorskie należą do 2022 Royal Society of Chemistry

The crystal structure of halide double perovskites is similar to the traditional perovskite structure, characterized by a cubic arrangement of oxygen atoms with cations located at the corners and center of the cube [61]. In contrast to ABX_3 perovskites, where the structure is formed solely by a B^{2+} centered octahedron, the structure of halide double perovskites is constructed with alternating B' and B" centered octahedra, specifically, $B'X_6$ and $B''X_6$, arranged in a three-dimensional framework as shown in Figure 1e.

The morphology of double perovskite materials can vary based on the synthesis method employed. Common techniques for preparing perovskite materials include solid-state reactions, hot injection, sol-gel methods, and chemical vapor deposition (see Table 1) [62–65]. Some typical morphologies observed for halide double perovskites include nanoparticles, nanocrystals, nanoplatelets, and quantum dots [64,66–70]. An in-depth understanding of the distinctive characteristics associated with each morphology is essential for tailoring double perovskite materials to specific applications.

The optical characteristics of halide double perovskites are derived from their efficacy in harvesting visible light. A comprehensive analysis of these optical properties involves various optoelectronic characterizations, including absorption coefficients, band gaps width, photoluminescence quantum yields, and lifetimes [71,72]. The energy band gap of a perovskite material demonstrates an inverse

relationship with its absorption threshold, implying that perovskites with higher band gaps typically display narrower absorption. Notably, perovskite materials commonly manifest both direct and indirect band gaps, contributing to their versatile optical behavior [73,74].

Double halide perovskites have been explored for various photocatalytic applications such as hydrogen generation [75,76], CO_2 reduction [77–79], pollutant degradations [80,81], and solar fuel production [82]. Ongoing researches are focused on employing diverse strategies, including composition modification, bang gap engineering, and the development of encapsulation techniques to improve photocatalytic performance of double halide perovskites [83–85]. For example, Zhang et al. developed $Cs_2AgBiBr_6$ double perovskite using a surface defect-induced electronic structure approach for efficient photocatalytic tetracycline degradation [86]. $Cs_2AgBiBr_6$ crystals precipitate rapidly with ethanol as the precipitant and EDTA as the chelating agent. The evaporation of water and strong ethylenediaminetetraacetic acid (EDTA) chelation with Cs^+ ions lead to the formation of numerous vacancies, creating surface defects and optimizing the electronic structure of the $Cs_2AgBiBr_6$ semiconductor. Wang et al. synthesized the $Cs_2AgBiBr_6$@g-C_3N_4 Z-scheme system in toluene and the $Cs_2AgBiBr_6$@g-C_3N_4 type II heterojunction in dichloromethane using an *in situ* assembly strategy on the $Cs_2AgBiBr_6$ surface [78]. These composites were evaluated for CO_2 photoconversion. The Z-scheme system, combining the reducing ability of g-C_3N_4 conduction band and the oxidizing ability of $Cs_2AgBiBr_6$ valence band, demonstrated superior CH_4 production in photocatalytic CO_2 reduction compared to the heterojunction photocatalysts, which exhibited high CO selectivity. Chen et al. prepared $Cs_2AgInCl_6$ quantum dots (QDs) with various Ag nanoparticles loading via hot-injection method for CO_2 reduction [66]. The authors used the surface plasmon resonance effect of Ag to improve the light absorption performance. As a result, the composite exhibited high conversion to CO and CH_4. Selected examples of double halide perovskites and their composites employed in photocatalytic applications are collected in Table 1.

Ensuring the stability of lead-free double perovskites is paramount for their successful implementation in practical applications. Studies have indicated that, in comparison to lead halide perovskites, double perovskites demonstrate enhanced stability against factors like oxygen, humidity, and temperature [60,72]. For example, Li et al. described formation of a stable $Cs_2AgInCl_2$ perovskite with octahedral particles, achieved through precipitation from acid solutions for the purpose of photocatalytic organic dye degradation [81]. The authors ascribed the improved photocatalytic efficiency to the perovskite's extended carrier lifetime and direct band gap . Furthermore, the strategic formation of a heterojunction represents a promising approach to enhance both the stability and photocatalytic properties of the material. Zhang et al. fabricated a MoS_2/$Cs_2AgBiBr_6$ heterostructure using a dissolution-recrystallization method, affixing non-noble MoS_2 onto $Cs_2AgBiBr_6$ [76]. The com-

posite displayed exceptional stability in photocatalytic hydrogen evolution reactions, showing no degradation over a 500-hour cyclic test. The enhanced performance was attributed to efficient photoinduced charge-carrier separation and transfer at the $MoS_2/Cs_2AgBiBr_6$ type I heterojunction. Additionally, the presence of edges and defects on/in MoS_2 nanoflowers supported by $Cs_2AgBiBr_6$ contributed to enriched reactive centers. Despite these favorable characteristics, the current levels of stability remain in need of refinement.

2. PHOTOCATALYTIC PERFORMANCE OF PEROVSKITE MATERIALS

Numerous studies have investigated the photocatalytic performance of perovskite materials for various applications in environmental and energy conversion, such as H_2 / O_2 evolution, CO_2 photoconversion, and pollutant degradation in both aqueous and gas phases. However, the structural instability and rapid recombination of electron-hole pairs present challenges. Consequently, researchers are actively exploring ways to enhance the photocatalytic performance of perovskite materials by tuning their composition, morphology, and surface properties. This includes the development of novel perovskite derivatives and double halide perovskites, as well as addressing stability and toxicity concerns. Advances in understanding the fundamental processes in perovskite photocatalysis contribute the ongoing optimization of these materials for practical applications in environmental and energy-related processes. Table 1 presents synthesis methods and highlights the photocatalytic performance of selected perovskite materials, providing insights into their potential applications and paving the way for further refinement in this field

Table 1.   Summary of the photocatalytic applications of perovskite materials in photocatalytic reactions. Synthesis method, and photocatalytic performance of the perovskite materials (type of model reaction, conditions, and photoactivity).

Tabela 1.   Podsumowanie fotokatalitycznych zastosowań materiałów perowskitowych w reakcjach fotokatalitycznych. Metoda syntezy oraz aktywność fotokatalityczna materiałów perowskitowych(rodzaj modelowej reakcji, warunki reakcji oraz wydajność).

Compound	Synthesis method	Type of model reaction	Photocatalytic performance		Ref.
			Conditions of the reaction (irradiation source and range, sample amount, environment, exposure time)	Efficiency/Yield/ Reaction rate	
Perovskite oxides					
CaTiO$_3$-Pt	Hydrothermal	H$_2$/O$_2$ evolution	500 W Hg lamp / UV / 0.5 g / 20 ml 0.2 M NaOH aqueous solution / 5 h	H$_2$: 130 µmol O$_2$: 50 µmol	[26]
NaNbO$_3$	Pulsed laser ablation	RhB degradation	300 W Xe lamp / UV-vis / the sample with the area of 1 cm^2 in a 1 mL RhB aqueous solution/ 1 h	70% photodegradation (C_0 = 2.5 mg L^{-1})	[30]
La-Doped NaTaO$_3$	Solid state	H$_2$/O$_2$ evolution	300 W Xe lamp / UV-vis / 0.1 g / 10 mL water / time not given	H$_2$: 90 µmol h^{-1} O$_2$: 45 µmol h^{-1}	[87]
Cr-Doped SrTiO$_3$	Microwave-assisted solvothermal	NO degradation	2.5 W LED / λ = 627 nm / not given / 1 ppm NO-50 vol.% air (balanced N$_2$) mixed gas (flow rate: 200 cm^3 min^{-1}) / 70 min	20% degradation at 10 min	[28]
NaTaO$_3$	Solid state	CO$_2$ conversion	4 UV fluorescent lamps of 6 W each / λ$_{max}$ = 365 nm / 0.1 g / 280 ml CO$_2$:H$_2$O molar ratio of 7.25 / 15 h	CO: 4 µmol g^{-1} h^{-1} CH$_4$: 0.16 µmol g^{-1} h^{-1} CH$_3$OH: 0.2 µmol g^{-1} h^{-1}	[88]
BiFeO$_3$	Sol-gel	MO degradation	300 W Xe lamp / λ > 420 nm / 30 mmol L^{-1} in MO aqueous solution / 16 h	90% photodegradation (C_0 = 15 mg L^{-1})	[36]
LaNiO$_3$/CdS	Hydrothermal	H$_2$ evolution	300 W Xe lamp / λ > 420 nm / 20 mg / 80 mL 0.1 M Na$_2$S/Na$_2$SO$_3$ / 3 h	3700 µmol g^{-1} h^{-1}	[37]
SrTiO$_3$/NiP	Hydrothermal	H$_2$ evolution	LED / λ = 427 nm / 2 mg / 20 mL methanol aqueous solution / time not given	5133.93 µmol g^{-1}	[89]

Halide perovskites derivates

Material	Method	Application	Conditions	Results	Ref.
Fe(II)-doped CsPbBr$_3$	Hot-injection	CO$_2$ conversion	450 W Xe lamp / 5 mg / CO$_2$:H$_2$O vapor / 3 h	<u>undoped CsPbBr$_3$:</u> CO 4.6 μmol·g^{-1}·h^{-1}, CH$_4$ 1.9 μmol·g^{-1}·h^{-1}; <u>Fe(II)-doped CsPbBr$_3$:</u> CO 3.2 μmol·g^{-1}·h^{-1}, CH$_4$ 6.1 μmol·g^{-1}·h^{-1}	[48]
CsPbBr$_3$@ZIFs	LARP/ in situ crystallization	CO$_2$ conversion	100 W Xe lamp / AM 1.5G filter / 4.5 mg / CO$_2$:H$_2$O vapor / 3 h	<u>CsPbBr$_3$@ZIF-8</u> CO 1.561 μmol·g^{-1}, CH$_4$ 5.434 μmol·g^{-1}; <u>CsPbBr$_3$@ZIF-67</u> CO 2.301 μmol·g^{-1}, CH$_4$ 10.537 μmol·g^{-1}	[49]
(CH$_3$NH$_3$)$_3$Bi$_2$I$_9$/ Pt	Recrystallization from HI saturated solution	H$_2$ evolution	300 W Xe lamp / 400 nm cut-off filter, Pt (2mg) / (CH$_3$NH$_3$)$_3$Bi$_2$I$_9$ (40 mg), HI perovskite saturated aqueous solution / 10 h	<u>(CH$_3$NH$_3$)$_3$Bi$_2$I$_9$/Pt</u> H$_2$ 169.21 μmol·g^{-1}·h^{-1} <u>(CH$_3$NH$_3$)$_3$Bi$_2$I$_9$</u> H$_2$ 12.19 μmol·g^{-1}·h^{-1}	[50]
Cs$_3$Bi$_2$ (Cl/Br)$_9$/C$_3$N$_4$	LARP/physical adsorption with thermal treatment	Phenol degradation	1000 W Xe lamp / cut-off filter below 420 nm or 455 nm / 6 g/L / 20 mg·L^{-1} phenol solution / 4 h	Vis (420 nm) – 84% Vis (455 nm) – 35%	[59]
A$_3$Bi$_2$I$_9$ type (A = Cs, Rb, MA, FA)	LARP	H$_2$ evolution	1000 W Xe lamp / without (UV) or with optical cut-off filter below 420 nm / 1.25 g·L^{-1} / HI/H$_3$PO$_2$, perovskite saturated aqueous solution or 10 vol.% methanolic aqueous electrolyte / 4 h	<u>Under UV in HI/H$_3$PO$_2$:</u> Cs$_3$Bi$_2$I$_9$ –2304 μmol·g$_{\text{sat.}}^{-1}$, Rb$_3$Bi$_2$I$_9$– 481.6 μmol·g$_{\text{sat.}}^{-1}$, MA$_3$Bi$_2$I$_9$–170.4 μmol·g$_{\text{sat.}}^{-1}$, FA$_3$Bi$_2$I$_9$–161.8 μmol·g$_{\text{sat.}}^{-1}$; <u>Under Vis in HI/H$_3$PO$_2$:</u> Cs$_3$Bi$_2$I$_9$–10.5 μmol/g$_{\text{sat.}}$; <u>Under UV in 10 vol. % MeOH:</u> Cs$_3$Bi$_2$I$_9$ –35.5 μmol·g$_{\text{cat.}}^{-1}$	[53]

Material	Method	Reaction	Conditions	Performance	Ref.
$CsPbBr_3/TiO_2$	Wet impregnation	Conversion of benzyl alcohol to benzaldehyde	300 W Xe lamp / cut-off filter below 420 nm / 25 mg / 5 mL of 0.1 M benzyl alcohol solution in toluene / 20 h	$Rb_3Bi_2I_9$ –31.7 $\mu mol \cdot g_{cat.}^{-1}$ $MA_3Bi_2I_9$–24.1 $\mu mol \cdot g_{cat.}^{-1}$ $FA_3Bi_2I_9$ – 20.1 $\mu mol \cdot g_{cat.}^{-1}$ 50% conversion	[90]
$Cs_3Bi_2Br_9$/polyt hiophene	LARP/in situ polymerization on perovskite surface	Degradation of toluene in gas phase	UV-LEDs / λ_{max} = 365 nm / 20 mg / toluene 50 ppm / 1 h	39.8%	[51]
$CsPbBr_3/GO$	LARP /modified Hammers' method	CO_2 conversion	1000 W Xe lamp / AM 1.5G filter / 4 mg / ethyl acetate / 12 h	CO 58.7 $\mu mol \cdot g_{cat.}^{-1}$ CH_4 29.6 $\mu mol \cdot g_{cat.}^{-1}$ H_2 1.58 $\mu mol \cdot g_{cat.}^{-1}$	[91]
$DMASnBr_3/C_3N_4$	Ball milling/thermal polymerization	H_2 evolution	1500 W Xe lamp / UV outdoor filter made of IR-treated soda lime glass / 1 g L^{-1} / 10% (v/v) TEOA, Pt 3 wt% / 6 h	1700 $\mu mol \cdot g^{-1} \cdot h^{-1}$	[92]

Double halide perovskites

Material	Method	Reaction	Conditions	Performance	Ref.
$Cs_2AgBiBr_6$	Hydrobromic acid precipitation and antisolvent recrystallization	TC degradation	300 W Xe lamp / AM 1.5 G filter / 0.02g / 0.05 /L TC ethanol solution / 90 min	81.8%	[86]
$Cs_2AgBiBr_6$	Hot-injection	CO_2 conversion	100 W Xe lamp / AM 1.5 G filter / 15 mg / 10 mL of ethyl acetate / 6 h	14.1 $\mu mol\ g^{-1}$ CO, 9.6 $\mu mol\ g^{-1}$ CH_4, ~70% CH_4	[77]
$Cs_2AgBiBr_6/g$-C_3N_4	*in situ* assembly	CO_2 conversion	150 mW cm^{-2} / 15 mg / 4 mL of ethyl acetate and 1 mL of methanol / time not given		[78]
$Cs_2AgBiBr_6/$ bismuthene composites	LARP	CO_2 conversion	300 W Xe / AM1.5G filter / 7 mg / 35 mL anhydrous methanol / 2 h	CH_4: 1.49(±0.16) $\mu mol\ g^{-1}\ h^{-1}$, CO: 0.67(±0.14) $\mu mol\ g^{-1}\ h^{-1}$, H_2: 0.75(±0.20) $\mu mol\ g^{-1}\ h^{-1}$	[79]

Material	Method	Application	Conditions	Performance	Ref.
$Cs_2AgBiBr_6$/ $Mo_3S_{13}^{2-}$	Hydrobromic acid precipitation and antisolvent recrystallization	H_2 evolution	300 W Xe / cutoff filter >420 nm / 0.5 g / 10 mL HBr saturated solution / 10 h	24.7 $\mu mol\ g^{-1}$	[75]
$Cs_2AgBiBr_6$/ MoS_2	Dissolution - recrystallization	H_2 evolution	300 mW cm^{-2} / $\lambda \geq$ 420 nm / 50 mg / 5 mL HBr/H_3PO_2 saturated / not given	87.5 $\mu mol\ g^{-1}\ h^{-1}$	[76]
$Cs_2AgBiCl_6$	Hydrochloric acid precipitation and antisolvent recrystallization	Sudan III degradation	300 W Xe / $\lambda \geq$ 400nm / 15mg / 30 mg·L^{-1} / 10 min	95.7 %	[80]
$Cs_2AgInCl_6$	Hydrochloric acid precipitation	Sudan Red III, RhB, MO, MR degradation	300 W Mercury lamp / UV-light / 20 mg / 10 mg·L^{-1} / not given	98.5% Sudan Red III (16 min) 91.7% MO (60 min) 92.9% MR (70 min) 90.8% RhB (140 min)	[81]
$Cs_2AgInCl_6$/Ag	Hot-injection	CO_2 conversion	300 W Xe / Vis irradiation / 10 mg / 20 mL of ethanol / 3 h	26.4 $\mu mol\ g^{-1}$ CO, 28.9 $\mu mol\ g^{-1}$ CH$_4$	[66]

CONCLUSIONS

In this review, we briefly summarized the preparation methods, properties, and photocatalytic performance of diverse perovskite structures, perovskite oxides, halide perovskite derivatives, and double halide perovskites. It is important to note that while perovskite materials show great potential, there are still challenges such as stability and toxicity concerns that need to be addressed for their widespread application in photocatalysis. Therefore, we hope that ongoing research aims to optimize these materials and explore new perovskite compositions to enhance their photocatalytic performance.

ACKNOWLEDGMENT

REFERENCES

[1]   E.A. Katz, Helv. Chim. Acta, 2020, **103**, e2000061.
[2]   G. Rose, Ann. Phys., 1839, **124**, 551.
[3]   B. Diouf, A. Muley, R. Pode, Energies, 2023, **16**,.
[4]   S.A. Khandy, D.C. Gupta, J. Magn. Magn. Mater., 2018, **458**, 176.
[5]   Q. Mahmood, S.A. Ali, M. Hassan, A. Laref, Mater. Chem. Phys., 2018, **211**, 428.
[6]   Y. Wu, L. Qiu, J. Liu, M. Guan, Z. Dai, G. Li, Adv. Opt. Mater., 2022, **10**, 2102661.
[7]   J.Y. Kim, J.-W. Lee, H.S. Jung, H. Shin, N.-G. Park, Chem. Rev., 2020, **120**, 7867.
[8]   Z. Jia, C. Cheng, X. Chen, L. Liu, R. Ding, J. Ye, J. Wang, L. Fu, Y. Cheng, Y. Wu, Mater. Adv., 2022, **4**, 79.
[9]   M. Irshad, Q. tul Ain, M. Zaman, M.Z. Aslam, N. Kousar, M. Asim, M. Rafique, K. Siraj, A.N. Tabish, M. Usman, M. ul Hassan Farooq, M.A. Assiri, M. Imran, RSC Adv., 2022, **12**, 7009.
[10]   A. Kumar, A. Kumar, V. Krishnan, ACS Catal., 2020, **10**, 10253.
[11]   S. Behara, T. Poonawala, T. Thomas, Comput. Mater. Sci., 2021, **188**, 110191.
[12]   X. Ye, X. Wang, Z. Liu, B. Zhou, L. Zhou, H. Deng, Y. Long, Dalt. Trans., 2022, **51**, 1745.
[13]   P.M. Bulemo, I.D. Kim, J. Korean Ceram. Soc., 2020, **57**, 24.
[14]   J. Park, W.A. Saidi, B. Chorpening, Y. Duan, Chem. Mater., 2022, **34**, 6108.
[15]   Q. Wang, Z. Chen, Y. Chen, N. Cheng, Q. Hui, Ind. Eng. Chem. Res., 2012, **51**, 11821.
[16]   Y. Zhang, Q. Zhong, Y. Bu, D. Meng, H. Gu, Q. Lu, Y. Zhao, G. Zhu, Energy and Fuels, 2021, **35**, 17353.
[17]   J. Mi, J. Chen, X. Chen, X. Liu, J. Li, Chem. - A Eur. J., 2023, **29**,.
[18]   V.-H. Nguyen, H.H. Do, T. Van Nguyen, P. Singh, P. Raizada, A. Sharma, S.S. Sana, A.N. Grace, M. Shokouhimehr, S.H. Ahn, C. Xia, S.Y. Kim, Q. Van Le, Sol. Energy, 2020, **211**, 584.
[19]   G. Li, M. Li, R. Taylor, Y. Hao, G. Besagni, C.N. Markides, Appl. Therm. Eng., 2022, **209**, 118285.
[20]   K. Maeda, M. Eguchi, T. Oshima, Angew. Chemie Int. Ed., 2014, **53**, 13164.
[21]   M. Roudgar-Amoli, E. Abedini, A. Alizadeh, Z. Shariatinia, J. Ind. Eng. Chem., 2024, **129**, 579.
[22]   S. Zeng, P. Kar, U.K. Thakur, K. Shankar, Nanotechnology, 2018, **29**,.
[23]   J. Wang, T. Wang, Z. Zhao, R. Wang, C. Wang, F. Zhou, S. Li, L. Zhao, M. Feng, J. Alloys Compd., 2022, **902**, 163865.
[24]   A. Zaleska-Medynska, Metal Oxide-Based Photocatalysis: Fundamentals and Prospects for Application, Elsevier, 2018.
[25]   R.I. Walton, Chem. - A Eur. J., 2020, **26**, 9041.

[26] H. Mizoguchi, K. Ueda, M. Orita, S.-C. Moon, K. Kajihara, M. Hirano, H. Hosono, Mater. Res. Bull., 2002, **37**, 2401.
[27] C. Wattanawikkam, T. Kansa-ard, W. Pecharapa, Appl. Surf. Sci., 2019, **474**, 169.
[28] U. Sulaeman, S. Yin, T. Sato, Appl. Catal. B Environ., 2011, **105**, 206.
[29] Y. Goto, T. Hisatomi, Q. Wang, T. Higashi, K. Ishikiriyama, T. Maeda, Y. Sakata, S. Okunaka, H. Tokudome, M. Katayama, S. Akiyama, H. Nishiyama, Y. Inoue, T. Takewaki, T. Setoyama, T. Minegishi, T. Takata, T. Yamada, K. Domen, Joule, 2018, **2**, 509.
[30] G. Li, Z. Yi, Y. Bai, W. Zhang, H. Zhang, Dalt. Trans., 2012, **41**, 10194.
[31] M. Passi, B. Pal, Powder Technol., 2021, **388**, 274.
[32] H. Zhang, G. Chen, Y. Li, Y. Teng, Int. J. Hydrogen Energy, 2010, **35**, 2713.
[33] H. Yang, C. Han, X. Xue, J. Environ. Sci., 2014, **26**, 1489.
[34] M. Passi, B. Pal, Korean J. Chem. Eng., 2022, **39**, 942.
[35] T. Soltani, X. Zhu, A. Yamamoto, S.P. Singh, E. Fudo, A. Tanaka, H. Kominami, H. Yoshida, Appl. Catal. B Environ., 2021, **286**, 119899.
[36] F. Gao, X.Y. Chen, K.B. Yin, S. Dong, Z.F. Ren, F. Yuan, T. Yu, Z.G. Zou, J.-M. Liu, Adv. Mater., 2007, **19**, 2889.
[37] J. Xu, C. Sun, Z. Wang, Y. Hou, Z. Ding, S. Wang, Chem. - A Eur. J., 2018, **24**, 18512.
[38] S. Mazumdar, Y. Zhao, X. Zhang, Front. Electron., 2021, **2**, 1.
[39] H. Nishiyama, T. Yamada, M. Nakabayashi, Y. Maehara, M. Yamaguchi, Y. Kuromiya, Y. Nagatsuma, H. Tokudome, S. Akiyama, T. Watanabe, R. Narushima, S. Okunaka, N. Shibata, T. Takata, T. Hisatomi, K. Domen, Nature, 2021, **598**, 304.
[40] T. Takata, J. Jiang, Y. Sakata, M. Nakabayashi, N. Shibata, V. Nandal, K. Seki, T. Hisatomi, K. Domen, Nature, 2020, **581**, 411.
[41] Q.A. Akkerman, L. Manna, ACS Energy Lett., 2020, **5**, 604.
[42] W. Ke, M.G. Kanatzidis, Nat. Commun., 2019, **10**, 1.
[43] P. Nandigana, S. Pari, D. Sujatha, M. Shidhin, C. Jeyabharathi, S.K. Panda, ChemistrySelect, 2023, **8**, e202204731.
[44] C. He, X. Liu, Light Sci. Appl., 2023, **12**, 15.
[45] K. Ren, S. Yue, C. Li, Z. Fang, K.A.M. Gasem, J. Leszczynski, S. Qu, Z. Wang, M. Fan, J. Mater. Chem. A, 2022, **10**, 407.
[46] F. Temerov, Y. Baghdadi, E. Rattner, S. Eslava, ACS Appl. Energy Mater., 2022, **5**, 14605.
[47] B. Li, S. Li, J. Gong, X. Wu, Z. Li, D. Gao, D. Zhao, C. Zhang, Y. Wang, Z. Zhu, Chem, 2024, **10**, 35.
[48] S. Shyamal, S.K. Dutta, N. Pradhan, J. Phys. Chem. Lett., 2019, **10**, 7965.
[49] Z.-C. Kong, J.-F. Liao, Y.-J. Dong, Y.-F. Xu, H.-Y. Chen, D.-B. Kuang, C.-Y. Su, ACS Energy Lett., 2018, **3**, 2656.
[50] Y. Guo, G. Liu, Z. Li, Y. Lou, J. Chen, Y. Zhao, ACS Sustain. Chem. Eng., 2019, **7**, 15080.
[51] M. Miodyńska, O. Kaczmarczyk, W. Lisowski, A. Żak, T. Klimczuk, M. Paszkiewicz, A. Zaleska-Medynska, Appl. Surf. Sci., 2024, **643**, 158725.
[52] Z. Jin, Z. Zhang, J. Xiu, H. Song, T. Gatti, Z. He, J. Mater. Chem. A, 2020, **8**, 16166.
[53] M. Miodyńska, T. Klimczuk, W. Lisowski, A. Zaleska-Medynska, Catal. Commun., 2023, **177**, 106656.
[54] Y. Cui, L. Yang, X. Wu, J. Deng, X. Zhang, J. Zhang, J. Mater. Chem. C, 2022, **10**, 16629.
[55] C. Tedesco, L. Malavasi, Molecules, 2023, **28**,.
[56] Y. Tang, C.H. Mak, C. Wang, Y. Fu, F.-F. Li, G. Jia, C.-W. Hsieh, H.-H. Shen, J.C. Colmenares, H. Song, M. Yuan, Y. Chen, H.-Y. Hsu, Small Methods, 2022, **6**, 2200326.
[57] S.S. Bhosale, A.K. Kharade, E. Jokar, A. Fathi, S. Chang, E.W.-G. Diau, J. Am. Chem. Soc., 2019, **141**, 20434.
[58] V.H. Nguyen, T. Lee, T.D. Nguyen, ACS Appl. Nano Mater., 2023, **6**, 3435.
[59] M. Miodyńska, A. Mikolajczyk, P. Mazierski, T. Klimczuk, W. Lisowski, G. Trykowski, A. Zaleska-Medynska, Appl. Surf. Sci., 2022, **588**, 152921.
[60] S. Ghosh, H. Shankar, P. Kar, Mater. Adv., 2022, 3742.
[61] O.A. Lozhkina, A.A. Murashkina, M.S. Elizarov, V. V. Shilovskikh, A.A. Zolotarev, Y. V. Kapitonov, R. Kevorkyants, A. V. Emeline, T. Miyasaka, Chem. Phys. Lett., 2018, **694**, 18.
[62] M. Cernea, F. Vasiliu, C. Plapcianu, C. Bartha, I. Mercioniu, I. Pasuk, R. Lowndes, R. Trusca, G. V. Aldica, L. Pintilie, J. Eur. Ceram. Soc., 2013, **33**, 2483.
[63] D.J. Kubicki, M. Saski, S. Macpherson, K. Gałkowski, J. Lewiński, D. Prochowicz, J.J. Titman, S.D. Stranks, Chem. Mater., 2020, **32**, 8129.
[64] D. Wu, Y. Tao, Y. Huang, B. Huo, X. Zhao, J. Yang, X. Jiang, Q. Huang, F. Dong, X. Tang, J. Catal., 2021, **397**, 27.
[65] R. Chahal, A. Bora, P.K. Giri, ACS Appl. Energy Mater., 2023, **6**, 8794.
[66] T. Chen, M. Zhou, W. Chen, Y. Zhang, S. Ou, Y. Liu, Sustain. Energy Fuels, 2021, **5**, 3598.

[67]   M.D.I. Bhuyan, S. Das, M.A. Basith, J. Alloys Compd., 2021, **878**, 2.
[68]   A. Schmitz, L. Leander Schaberg, S. Sirotinskaya, M. Pantaler, D.C. Lupascu, N. Benson, G. Bacher, ACS Energy Lett., 2020, **5**, 559.
[69]   Z. Liu, H. Yang, J. Wang, Y. Yuan, K. Hills-Kimball, T. Cai, P. Wang, A. Tang, O. Chen, Nano Lett., 2021, **21**, 1620.
[70]   Z. Chen, X. Li, Y. Wu, A. Duan, D. Wang, Q. Yang, Y. Fan, Sep. Purif. Technol., 2022, **302**, 122079.
[71]   H. Mai, D. Chen, Y. Tachibana, H. Suzuki, R. Abe, R.A. Caruso, Chem. Soc. Rev., 2021, **50**, 13692.
[72]   E. Meyer, D. Mutukwa, N. Zingwe, R. Taziwa, Metals (Basel)., 2018, **8**,.
[73]   Y. Cai, Z. Lu, X. Xu, Y. Gao, T. Shi, X. Wang, L. Shui, Materials (Basel)., 2023, **16**,.
[74]   T.T. Tran, J.R. Panella, J.R. Chamorro, J.R. Morey, T.M. McQueen, Mater. Horizons, 2017, **4**, 688.
[75]   Z. He, Q. Tang, X. Liu, X. Yan, K. Li, D. Yue, Energy and Fuels, 2021, **35**, 15005.
[76]   Y. Zhang, Z. Sun, Z. Wang, Y. Zang, X. Tao, Int. J. Hydrogen Energy, 2022, **47**, 8829.
[77]   L. Zhou, Y.F. Xu, B.X. Chen, D. Bin Kuang, C.Y. Su, Small, 2018, **14**, 1.
[78]   Y. Wang, H. Huang, Z. Zhang, C. Wang, Y. Yang, Q. Li, D. Xu, Appl. Catal. B Environ., 2021, **282**,.
[79]   M.S. Sena, J. Cui, Y. Baghdadi, E. Rattner, M. Daboczi, A.L. Lopes-Moriyama, A.G. dos Santos, S. Eslava, ACS Appl. Energy Mater., 2023, **6**, 10193.
[80]   K. Guo, P. Lin, D. Wu, Z. Shi, X. Chen, Y. Han, Y. Tian, X. Li, Chem. - A Eur. J., 2023, **29**, 2.
[81]   K. Li, S. Li, W. Zhang, Z. Shi, D. Wu, X. Chen, P. Lin, Y. Tian, X. Li, J. Colloid Interface Sci., 2021, **596**, 376.
[82]   S. Peng, Z. Yang, M. Sun, L. Yu, Y. Li, Adv. Mater., 2023, **35**, 2304711.
[83]   S. Purohit, S. Shyamal, S.K. Saini, K.L. Yadav, M. Kumar, S. Satapathi, Energy and Fuels, 2022, **36**, 12170.
[84]   L. Wu, S. Zheng, H. Lin, S. Zhou, A. Mahmoud Idris, J. Wang, S. Li, Z. Li, J. Colloid Interface Sci., 2023, **629**, 233.
[85]   P. Han, C. Luo, W. Zhou, J. Hou, C. Li, D. Zheng, K. Han, J. Phys. Chem. C, 2021, **125**, 11743.
[86]   S. Zhang, Y. Yuan, J. Gu, X. Huang, P. Li, K. Yin, Z. Xiao, D. Wang, Appl. Surf. Sci., 2023, **609**, 155446.
[87]   H. Sudrajat, M. Kitta, R. Ito, S. Nagai, T. Yoshida, R. Katoh, B. Ohtani, N. Ichikuni, H. Onishi, J. Phys. Chem. C, 2020, **124**, 15285.
[88]   F. Fresno, P. Jana, P. Reñones, J.M. Coronado, D.P. Serrano, V.A. De La Peña O'Shea, Photochem. Photobiol. Sci., 2017, **16**, 17.
[89]   J. Xie, P. Bai, C. Wang, N. Chen, W. Chen, M. Duan, H. Wang, ACS Appl. Energy Mater., 2022, **5**, 9559.
[90]   S. Schünemann, M. van Gastel, H. Tüysüz, ChemSusChem, 2018, **11**, 2057.
[91]   Y.-F. Xu, M.-Z. Yang, B.-X. Chen, X.-D. Wang, H.-Y. Chen, D.-B. Kuang, C.-Y. Su, J. Am. Chem. Soc., 2017, **139**, 5660.
[92]   L. Romani, A. Speltini, F. Ambrosio, E. Mosconi, A. Profumo, M. Marelli, S. Margadonna, A. Milella, F. Fracassi, A. Listorti, F. De Angelis, L. Malavasi, Angew. Chemie Int. Ed., 2021, **60**, 3611.